BIOCHEMISTRY
including biophysical chemistry & molecular biology
Article

Biochemistry **2009,** *48,* 6783–6793 6783
DOI: 10.1021/bi900530v

Phosphorylation of a Borealin Dimerization Domain Is Required for Proper Chromosome Segregation‡

Eric Bourhis,[§,⊥] Andreas Lingel,[§,⊥] Qui Phung,[∥] Wayne J. Fairbrother,[§] and Andrea G. Cochran*[,§]

[§]*Departments of Protein Engineering and* [∥]*Protein Chemistry, Genentech, Inc., 1 DNA Way, South San Francisco, California 94080* [⊥]*These authors contributed equally to this work*

Received March 27, 2009; Revised Manuscript Received May 27, 2009

ABSTRACT: The chromosomal passenger complex (CPC) has been identified as a master regulator of mitosis. In particular, proper chromosome segregation and cytokinesis depend on the correct localization and function of the CPC. Within the complex, the kinase Aurora B associates with Incenp, Survivin, and Borealin. The stoichiometry of the complex as well as a complete understanding of how these four components interact with each other remains to be elucidated. Here, we identify a new domain of Borealin. We determined its structure using NMR spectroscopy and discovered a novel dimerization motif. Interestingly, we found that substitutions at Borealin T230, recently identified as an Mps1 phosphorylation site, can modulate the dimerization state of Borealin. Mutation of this single residue to alanine or valine impairs Aurora B activity during mitosis and causes chromosome segregation defects. This study reveals that Mps1 regulates the CPC through a novel Borealin domain.

Accurate segregation of chromosomes during mitosis is necessary to ensure that all cells receive an exact copy of replicated genetic information. A key monitoring mechanism is the spindle assembly checkpoint (SAC)[1] whose function is to delay anaphase until all chromatids are properly bioriented and attached to the mitotic spindle (*1*). The chromosomal passenger complex (CPC), composed of Aurora B, Survivin, Borealin, and Incenp, has been shown to be a major contributor to the SAC. Additionally, the CPC contributes to chromatin condensation and kinetochore maturation, and it plays an important role during cytokinesis (for review, see refs *2* and *3*). The CPC displays a very particular pattern of localization: it is localized along the chromosome arms during early mitosis; then it accumulates at the centromeres during late prophase where it stays until anaphase onset. At this time, while chromosomes are being pulled to each pole of the cell, the CPC remains at the spindle midzone, and it slowly concentrates at the midbody until completion of cytokinesis.

Although the movement of the CPC yields striking visual clues about what it might do, the biochemical details are not well understood. In large part, this is because of a strict requirement that the CPC localize for each of its functions. In particular, knockdown of any one subunit leads to mislocalization of all the other subunits, resulting in dramatic mitotic defects (*4*−*6*). In addition, posttranslational modifications (many of unknown functional importance) have been reported for each of the individual subunits (*3*). This degree of complexity has complicated efforts to assign particular functions to individual proteins, domains, or subcomplexes of the CPC. *In vitro* reconstitution of the intact complex has not yet been achieved, and therefore significant details of the CPC structure, molecular organization, and stoichiometry are missing. On the other hand, recent structural studies of individual domains of CPC proteins or of CPC subcomplexes are revealing useful new insights into function.

A major role of the CPC is to target the kinase Aurora B to the correct sites of action. Aurora B interacts with the conserved C-terminal IN-box peptide of the large scaffold protein Incenp. This interaction not only tethers but also activates the kinase (*7*, *8*). Incenp binds to Survivin and Borealin through its helical N-terminal peptide (*9*, *10*). Survivin was the first of the CPC subunits to be structurally characterized (*11*−*13*) and forms a "bow tie-shaped" homodimer in solution. However, recent crystal structures show that when bound to Borealin, Survivin is a monomer (*9*, *14*). Survivin is composed of two important domains: the baculoviral inhibitory repeat (BIR) domain that is necessary, but not sufficient, for correct centromeric targeting (*15*, *16*) and a long helical extension that interacts with Borealin and Incenp (*9*, *14*). This latter region is sufficient for spindle midzone and midbody localization (*15*).

Borealin is the most recently identified CPC component (*4*, *17*), but, unlike Aurora B and Survivin, it contains no recognizable domains for which a function might be inferred. Borealin may

‡The coordinates and the NMR data for the Borealin 207−280 domain have been deposited under the file name "Solution structure of the conserved C-terminal dimerization domain of Borealin" at the Protein Data Bank and the BioMagResBank under accession numbers 2kdd and 16110, respectively.

*Corresponding author: Phone: 650-225-5943; Fax: 650-225-3734; E-mail: andrea@gene.com.

[1]Abbreviations: APC, anaphase promoting complex; ATP, adenosine triphosphate; BIR, baculoviral inhibitory repeat; CPC, chromosomal passenger complex; CENP-A, centromeric protein A; GFP, green fluorescent protein; HSQC, heteronuclear single-quantum coherence; IPTG, isopropyl β-D-1-thiogalactopyranoside; MBP, maltose binding protein; MCC, mitotic checkpoint complex; Mps1, multipolar spindle 1; NTA, nitrilotriacetic acid; OD, optical density; PAGE, polyacrylamide gel electrophoresis; SAC, spindle assembly checkpoint; TCEP, tris(2-carboxyethyl)phosphine; TEV, tobacco etch virus.

Published on Web 06/17/2009

instead play an accessory role by stabilizing the Survivin−Incenp complex, as supported by the centromeric localization of a Survivin−Incenp fusion protein engineered to bypass Borealin function (*6*). However, this idea has been challenged by studies showing that the N-terminal half of Borealin, which forms a stable ternary complex with Survivin and Incenp, can localize CPC proteins to the spindle midzone and midbody but not to the centromeres (*4*, *9*). This suggests that, in addition to the Survivin BIR domain, the C-terminal half of Borealin is necessary for centromeric localization of the complex. Moreover, a recent study shows that the kinase Mps1 phosphorylates Borealin, which appears to activate Aurora B at the centromeres (*18*). Together, these results confer upon Borealin a more important role than passively linking Survivin to Incenp.

In the present study, we identify a previously unrecognized Borealin dimerization domain in the C-terminal half of the protein. We have determined the structure of this new dimerization motif by multidimensional heteronuclear NMR spectroscopy. One of the previously reported Mps1 phosphorylation sites of Borealin lies at the dimer interface. Mutation of this residue is sufficient to produce changes in Aurora B activity and chromosome segregation errors previously observed upon global mutation of Mps1 phosphorylation sites present in Borealin.

MATERIALS AND METHODS

Construction of Plasmids for Bacterial Expression. The gene for full-length human Survivin was subcloned in-frame with the N-terminal His_6 tag of the T7 expression vector pET-28 (kanR; EMD Biosciences). The gene for human Borealin was subcloned into pET21 (ampR; EMD Biosciences). C-Terminal subdomains of Borealin were amplified by PCR and cloned into a modified pET21 with an N-terminal GB1 tag (B1 domain of protein G) followed by a TEV protease cleavage site. Mutants were generated using the XL-2 QuickChange kit (Stratagene). Incenp 1−58 was cloned into a modified pET24b vector (KanR; EMD Biosciences) containing a N-terminal MBP tag. The region of the gene coding for the Mps1 kinase domain encompassing residues 510−857 (*19*) was cloned into pET21 in-frame with the C-terminal His_6 tag. DNA sequences of all inserts were fully verified.

Protein Expression and Purification. *Escherichia coli* cells of the BL21-DE3 pLysS Rosetta 2 strain (EMD Biosciences) were transformed with full-length or C-terminal Borealin constructs. Positive colonies were selected on 50 μg/mL carbenicillin or 50 μg/mL carbenicillin and 50 μg/mL kanamycin for cotransformation with Survivin. Single colonies were grown in LB broth at 37 °C under antibiotic selection until the culture density reached an OD_{600} of 0.5. For uniform ^{15}N or ^{15}N and ^{13}C labeling of the Borealin C-terminal domain, cells were grown in M9 minimal medium supplemented with $^{15}NH_4Cl$ either without or with [$^{13}C_6$] glucose, respectively. Expression was induced by addition of isopropyl β-D-1-thiogalactopyranoside (IPTG) to 0.8 mM final concentration, and the cultures were shaken overnight at 22 °C. Harvested cells expressing Borealin−Survivin complexes were lysed in 100 mL/L of culture of buffer A (50 mM Tris, pH 8, 500 mM NaCl, 0.1 mM TCEP, 10% glycerol), while those expressing Borealin C-terminal fragments were lysed in phosphate-buffered saline (PBS); in each case lysis was by passage through a microfluidizer (EmulsiFlex; Avestin). The soluble lysate of full-length complexes was loaded onto a Ni-NTA agarose column (Qiagen; 0.5 mL of resin/L of culture). The column was washed with 20 volumes of buffer A containing 5 mM imidazole, and the Borealin−Survivin complex was eluted with 5 volumes of buffer A containing 300 mM imidazole. The complexes were further purified by size-exclusion chromatography on Superdex S-200 (GE Healthcare) in buffer A and then concentrated to 2 mg/mL for light scattering experiments. Soluble lysates from expression of Borealin C-terminal fragments were loaded onto IgG Sepharose 6 Fast Flow resin (GE; 1 mL of resin/L of culture). The column was washed with 20 volumes of PBS, and the Borealin fragment was eluted in 1 mL fractions with 1 M glycine, pH 3. Borealin-containing fractions were combined, and the proteins were further purified by size-exclusion chromatography on Superdex S-200 equilibrated in PBS. The GB1 tag was removed by TEV protease cleavage overnight. Cleaved products were loaded onto a cation-exchange column (SP FF; GE) equilibrated in PBS at pH 7.2 and eluted with a gradient from 0.15 to 1 M NaCl in the same buffer. Fractions containing Borealin were then pooled and further purified by gel filtration on Superdex S-75 (GE Healthcare) equilibrated in PBS. Fractions of Borealin with a purity above 95% were then concentrated to 4 mg/mL for NMR analysis. Mps1 was expressed and purified as described above for the full-length Borealin−Survivin complex, except substituting 50 mM Tris, pH 8, 300 mM NaCl, and 0.1 mM TCEP for buffer A. To purify Incenp 1−58, cells were resuspended in lysis buffer containing 50 mM sodium phosphate, pH 8, 300 mM NaCl, 20 mM imidazole, and 5 mM β-mercaptoethanol and subsequently lysed using a microfluidizer (EmulsiFlex; Avestin). Cell lysates were incubated with Ni-NTA Superflow beads (Qiagen). After elution with 300 mM imidazole in lysis buffer, the buffer was exchanged to 50 mM sodium phosphate, pH 8, 300 mM NaCl, and 10 mM β-mercaptoethanol. The fusion protein was cleaved overnight by TEV protease and subsequently passed over a second Ni-NTA column to remove the cleaved MBP and uncleaved fusion protein. The flow-through containing Incenp 1−58 was concentrated and further purified by size-exclusion chromatography using a Superdex S-75 column equilibrated in the same buffer.

NMR Spectroscopy. NMR spectra of Borealin 207−280 were acquired at 26 °C on a Bruker DRX600 spectrometer with a cryogenic triple-resonance probe and a DRX800 spectrometer equipped with a room temperature triple-resonance probe. Spectra were processed with Topspin (Bruker) and NMRPipe (*20*). Spectral analysis was performed using the CCPN analysis software (*21*). The ^1H, ^{13}C, and ^{15}N chemical shifts were assigned by standard methods. Distance restraints were derived from ^{15}N- or ^{13}C-resolved three-dimensional NOESY spectra, in addition to a ^1H homonuclear two-dimensional spectrum. Intermolecular distance restraints between the subunits of the dimer were obtained from an ^{13}C-filtered, ^{13}C-edited three-dimensional NOE experiment on a sample containing 50% unlabeled and 50% ^{13}C, ^{15}N-labeled protein (*22*). All NOESY spectra were recorded with a mixing time of 100 ms. Restraints for the backbone angles ϕ and ψ were derived from $^3J(H^N,H\alpha)$ coupling constants and TALOS (*23*). To detect slowly exchanging amide protons, ^1H,^{15}N correlation experiments were performed on lyophilized protein after redissolving in D_2O. Stereospecific assignments of leucine and valine methyl groups were obtained using a 10% fractionally ^{13}C-labeled sample, as described (*24*). H^N-N residual dipolar couplings were measured using a spin-state-selective ^1H,^{15}N correlation experiment in a dilute liquid crystalline medium (*25*). Heteronuclear $\{^1H\}-^{15}N$ NOEs were measured on a ^{15}N-labeled Borealin sample at 26 °C and 800 MHz ^1H Larmor frequency and analyzed with the CCPN analysis software.

Table 1: Structural Statistics for the Solution Structure of Borealin 207−280

	⟨SA⟩[a]	⟨SA⟩$_{\text{water refined}}$[a]
no. of structural restraints		
NOE-derived distance restraints (per monomer)		
total (unambiguous/ambiguous)	1900 (1857/43)	
intramonomer	(1693/43)	
intermonomer	(164/43)	
dihedral restraints (per monomer)	86	
ϕ	43	
ψ	43	
violations		
rmsd from exptl restraints		
NOE distance restraints (Å)	0.0046 ± 0.0005	0.0085 ± 0.0006
dihedral restraints (deg)	0.15 ± 0.03	0.19 ± 0.08
NOE distance violations		
no. > 0.1 Å	0.7 ± 1.4	7.8 ± 3.2
no. > 0.2 Å	0	0.4 ± 0.8
dihedral violations		
no. > 1°	0.8 ± 1.1	2.3 ± 2.2
no. > 2°	0	0.3 ± 0.6
rmsd from idealized geometry		
bonds (Å)	0.00111 ± 0.00003	0.00335 ± 0.00006
angles (deg)	0.285 ± 0.002	0.461 ± 0.001
impropers (deg)	0.158 ± 0.004	1.273 ± 0.115
Q-factor for exptl residual dipolar coupling restraints[b]		
$^1D_{HN}$ (40 per monomer)	0.036 ± 0.003	0.098 ± 0.005
coordinate precision (Å)[c]		
backbone (dimer)	0.38 ± 0.09	0.57 ± 0.08
all heavy atoms (dimer)	0.88 ± 0.11	0.96 ± 0.07
backbone (monomer)	0.33 ± 0.07	0.49 ± 0.06
all heavy atoms (monomer)	0.85 ± 0.10	0.89 ± 0.06
stereochemistry[d]		
Ramachandran plot		
% in most favored regions	89.4 ± 3.0	91.4 ± 2.8
% in additionally allowed regions	10.6 ± 3.0	8.6 ± 2.8
energies (kcal mol^{-1})[e]		
E_{NOE}	4.1 ± 0.9	13.7 ± 1.9
E_{CDIH}	0.2 ± 0.1	0.4 ± 0.3
E_{bond}	2.8 ± 0.1	25.6 ± 1.0
E_{angles}	51.1 ± 0.8	135.3 ± 7.0
E_{impr}	4.3 ± 0.3	284.5 ± 50.7

[a] ⟨SA⟩ is an ensemble of the ten lowest energy solution structures of Borealin 207−280 (out of 100 calculated). The CNS E_{repel} function was used to simulate van der Waals interactions with an energy constant of 25.0 kcal mol^{-1} Å^{-4} using "PROLSQ" van der Waals radii. 1 kcal = 4.18 kJ. For ⟨SA⟩$_{\text{water refined}}$, the ensemble of ⟨SA⟩ structures was refined in a shell of water (*28*). [b] Quality factor for the RDC refinement (*46*). Residual dipolar couplings were applied with a final energy constant of 0.2 kcal mol^{-1} Hz^{-2} for an alignment tensor with an axial component of 13.16 Hz and a rhombicity of 0.48. [c] Coordinate precision is given as the Cartesian coordinate rmsd of the ten lowest energy structures in the NMR ensemble with respect to their mean structure for Borealin 226−277. [d] Structural quality was analyzed using PROCHECK (*29*) for Borealin residues 226−277. [e] NOESY-derived distance restraints were used with a soft square-well potential using an energy constant of 50 kcal mol^{-1} Å^{-2}. $^3J(H^N,H\alpha)$ coupling constants and TALOS (*23*) derived dihedral angle restraints and were applied to ϕ, ψ backbone angles using an energy constant of 200 kcal mol^{-1} rad^{-2}. The force constants were 1000 kcal mol^{-1} Å^{-2} for bond lengths and 500 kcal mol^{-1} rad^{-2} for angles and improper dihedrals.

Structure Calculation. The experimentally determined distance and dihedral angle restraints for Borealin 207−280 (see Table 1) were applied in a simulated annealing protocol using ARIA 2.2 (*26*) and CNS (*27*). Noncrystallographic symmetry restraints were used to enforce the dimer symmetry. The final ensemble of NMR structures was refined in a shell of water molecules (*28*). Structural quality was analyzed using PROCHECK (*29*). Ribbon representations were prepared with MOLMOL (*30*) and PyMOL (DeLano Scientific).

Light Scattering Analysis. Aliquots of 100 μL of protein at 1 mg/mL were centrifuged briefly, and the supernatant was analyzed by SEC-MALS (Agilent 1100 HPLC; Wyatt Technologies miniDawn TriStar and Optilab DSP). Samples were chromatographed at 1 mL/min in 50 mM Tris, pH 8, 500 mM NaCl, 0.1 mM TCEP, and 10% glycerol over an S200 Superdex 10/300 GL column (GE Healthcare). One microliter of each aliquot was also analyzed for protein content by SDS−PAGE (NuPAGE, 4−12% MES buffer; Invitrogen).

Circular Dichroism. Thermal denaturation of the Borealin C-terminal domain was monitored at 222 nm with a J-810 spectrometer (Jasco, Easton, MD), using a 10 mm path length cuvette containing protein samples (114 μM) in 50 mM potassium phosphate, pH 7.2, and 150 mM NaCl. The temperature was increased from 10 to 95 °C in steps of 1 °C per minute. The melting temperature (T_m) given corresponds to the inflection point of the major transition observed for each sample.

Tandem Mass Spectrometry. The Borealin−Survivin complex was treated with Mps1 and ATP (600 μg:300 μg at 1 mM ATP, sample 1, or 100 μg:20 μg at 200 μM ATP, samples 2 and 3) in 25 mM Tris-HCl, pH 7.5, 5 mM β-glycerophosphate, 2 mM dithiothreitol, 0.1 mM Na_3VO_4, and 10 mM $MgCl_2$ for 4 h at 30 °C. Treated complexes were digested at 37 °C overnight with

trypsin (Promega, 1:50 ratio) following reduction with dithiothreitol (10 mM; 50 °C for 40 min) and alkylation with iodoacetamide (10 mM; room temperature in the dark for 30 min). Excess iodoacetamide was quenched with 3 mM dithiothreitol in the dark at room temperature for 30 min. The protein digests were analyzed by capillary reversed-phase HPLC-ESI-MS/MS on a linear ion trap Fourier transform ion cyclotron resonance mass spectrometer (LTQ-FT; ThermoFisher). Samples were loaded in 0.1% formic acid in water onto a 100 μm i.d. capillary trapping column (IntegraFrit; New Objective) packed with 5 cm of C18 5 μm material (Michrom; Bioresources) and resolved using a 75 μm i.d. column (PicoFrit; New Objective) packed with 13 cm of the same material. Peptides were eluted with a 60 min gradient of 2−90% of 0.1% formic acid in acetonitrile at 250 nL/min generated by a microcapillary HPLC system (NanoLC-2D; Eksigent). Eluted peptides were introduced to the mass spectrometer by electrospray ionization through the application of a 1.7 kV potential to the PicoFrit emitter. Mass spectral data were acquired using a method comprising of one full MS scan (m/z 300−2000) followed by nine targeted product ion scans, such that each mass was successively subjected to collision-induced dissociation in a cycle repeated throughout the LC gradient. Ions chosen for targeted experiments included the doubly charged ions of the Borealin tryptic peptides containing T88, T169, and T230 in each of their potential phosphorylation states (maximum of two). The triply charged ion of the doubly phosphorylated peptide containing T88 was also included. Tandem mass spectral results were submitted for database searching using the Mascot program (Matrix Science) against both a Genentech protein database and the SwissProt database with 30 ppm precursor ion mass and 0.8 Da MS/MS tolerance. Phosphorylated peptide identifications were confirmed by manual interpretation of mass spectral data.

Transfection and Expression Analysis by Western Blot. HeLa cells (ATCC; CCL-2) grown in DMEM high-glucose medium in a 10 cm dish were transfected with 6 μg of plasmid using FuGENE 6 (DNA:FuGENE at ratio 1:3; Roche) for 6 h before the medium was replaced. At 20 h posttransfection, cells were washed two times with cold PBS and collected in 400 μL of lysis buffer (50 mM Tris, pH 7.5, 5% glycerol, 2.5 mM $MgCl_2$, 100 mM NaCl, 25 mM NaF, 1 mM Na_3VO_4, 0.05% NP-40). Whole-cell lysate from cells transfected with wild-type or mutant GFP−Borealin were loaded onto a 4−12% NuPAGE gel (Invitrogen) run in MES buffer. Proteins were transferred onto a nitrocellulose membrane which was then blocked overnight with 5% powdered milk and 0.05% Tween-20 in PBS. Antibodies used were mouse anti-GFP (1/1000; Invitrogen), rabbit anti-mouse HRP (1/2000; Invitrogen), and rabbit anti-β-tubulin HRP (1/10000; Abcam).

Immunofluorescence Microscopy. Wild-type full-length Borealin and the different mutants were each subcloned by PCR into pDONOR201 (Invitrogen) and fully sequenced. Genes were subsequently transferred into the vector pEF5-FRT-V5 (Invitrogen), which had been additionally modified with an N-terminal eGFP tag. HeLa cells (ATCC; CCL-2) were grown in DMEM high-glucose medium in 24-well glass plates for 20 h. Cells were then transfected with plasmid (0.2 μg) using FuGENE 6 (DNA:FuGENE at ratio 1:3; Roche) for 6 h. The medium was replaced with medium containing 2 mM thymidine or 200 ng/mL nocodazole, and the cells were incubated for an additional 16 h. Cells were then released from the thymidine block by replacement of the medium. After an additional 8 h, cells were fixed for 20 min by treatment with 4% paraformaldehyde in PBS. Fixed cells were washed two times for 10 min with PBS, permeabilized with 0.1% Triton X-100 in PBS for 5 min, and then blocked overnight in normal donkey serum (Jackson ImmunoResearch). Primary antibodies were mouse anti-Aurora B (BD Biosciences, 611082; 1:200), mouse anti-Survivin (Santa Cruz Biotechnology, sc-17779; 1:200), and rabbit anti-pSer7-CENP-A (Upstate; 1:400). These were diluted in donkey serum and added to blocked wells for 1 h. After washing, the appropriate secondary antibody conjugate (donkey anti-mouse Cy3 or goat anti-rabbit Cy3, 1:600; Jackson ImmunoResearch) was added for 45 min in the presence of Hoechst 33342 (Invitrogen; 1:30000). Cells were washed in PBS. Images were captured using an inverted IX-81 microscope (Zeiss) with a 60× objective and the acquisition program Slidebook (Intelligent Imaging Innovations). To quantify the levels of pSer7-CENP-A or GFP−Borealin for the experiment shown in Figure 5, average pixel intensities of regions encompassing centromeres were determined in the various channels and corrected by subtracting the cytoplasmic background intensity. A total of 23 cells from four different wells per condition were evaluated. To quantify the fraction of cells with lagging chromosomes for the experiment shown in Figure 4, an average of 95 cells per condition from four different transfection experiments were evaluated. Data are reported as average ± standard deviation.

RESULTS

Identification of a Borealin Dimerization Domain. The idea that Borealin might oligomerize *in vivo* was first suggested by the observed coimmunoprecipitation of HA-tagged Borealin and a cotransfected Myc-tagged Borealin (*10*). However, it was not determined whether the interaction is direct or which part of Borealin might be required. More recently, evidence has emerged that the N-terminus of Borealin might dimerize when it is present in a binary complex with Survivin (*9*, *14*). However, the oligomeric state of this complex, which has a stoichiometry of 2:2, changes upon addition of an excess of Incenp 1−58, yielding a new complex with 1:1:1 stoichiometry (*9*). This suggests that the N-terminus of Borealin would not support oligomerization within the intact CPC. In contrast, Zhou et al. report that the Borealin (13−92)−Survivin complex is not capable of binding to Incenp 1−69 (*31*).

We purified the binary complex of Survivin and full-length Borealin and determined its size-exclusion profile in the presence and absence of added Incenp 1−58 (Figure 1A). A complex of Survivin and a minimized binding fragment of Borealin encompassing residues 20−78 (*14*) was evaluated for comparison. In agreement with the earlier study (*9*), we observed a shift of the elution volume toward lower molecular weight upon addition of Incenp 1−58 to the Borealin (20−78)−Survivin complex, consistent with a change in stoichiometry from 2:2 to 1:1:1. In contrast, addition of the Incenp fragment to the complex of Survivin and full-length Borealin resulted in a ternary complex that elutes earlier than the binary complex (but clearly after the void volume), suggesting that the ternary complex is not of 1:1:1 stoichiometry. The shift to a higher molecular weight species when including the C-terminus of Borealin suggests that this additional part of the protein might contain a previously unrecognized oligomerization domain and that this might be the region responsible for the reported self-association of Borealin.

Aside from the N-terminal region that binds to Survivin and Incenp, Borealin is structurally uncharacterized. There is a

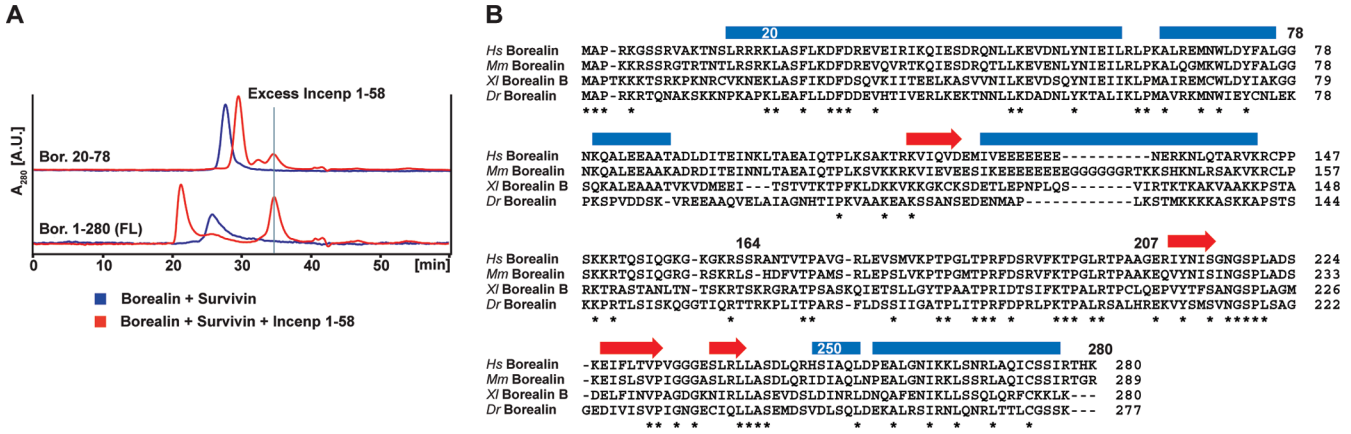

FIGURE 1: Identification of the Borealin dimerization domain. (A) Gel filtration profiles of Borealin 20−78 and full-length Borealin in complex with Survivin before (blue) and after (red) addition of an excess of Incenp 1−58. (B) Sequence alignment and secondary structure prediction for Borealin. Blue bars and red arrows indicate helices and strands predicted for the human sequence by Quick2D, respectively (MPI toolkit (*33*)). The sequence alignment was obtained using the program Clustal X (*47*), and completely conserved residues are indicated with an asterisk (*Hs*, *Homo sapiens*; *Mm*, *Mus musculus*; *Xl*, *Xenopus laevis*; *Dr*, *Danio rerio*).

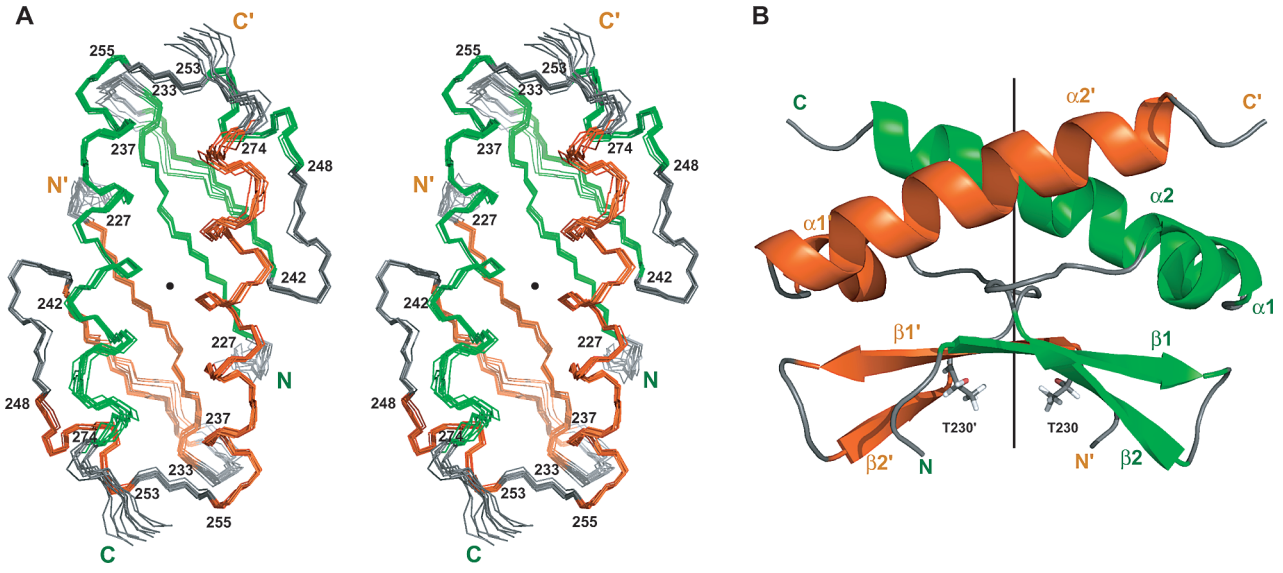

FIGURE 2: Solution structure of human Borealin 207−280. For clarity, only Borealin residues 224−277 are shown. (A) Stereoview of the ensemble of the ten lowest energy NMR structures of the Borealin 207−280 dimer. Secondary structural elements are colored in green and orange for the two subunits, respectively. The *C*2 symmetry axis is indicated by a black dot. (B) Ribbon representation of the Borealin 207−280 dimer in a view rotated by 90° rotations around both the *x* and *z* axis compared with (A). The critical T230 and the *C*2 symmetry axis are shown.

central, very hydrophilic segment followed by a C-terminal region whose sequence is more consistent with the presence of a structured domain. The sequence of this region is reasonably well conserved among species (Figure 1B), but we were unable to identify any known domains using primary sequence analysis programs such as SMART (*32*). However, several secondary structural elements could be predicted with reasonable confidence (Quick2D, MPI toolkit (*33*)), and these correspond to the more highly conserved motifs in the Borealin C-terminus. Four constructs were designed including different combinations of the predicted secondary structural motifs (Supporting Information Figure S1A). Those fragments of the Borealin C-terminus that could be obtained in soluble form were evaluated for evidence of structure by NMR. This analysis defined a relatively short folded sequence encompassing residues 207−280 (Supporting Information Figure S1B). This Borealin C-terminal fragment also showed a gel-filtration profile consistent with dimerization (Supporting Information Figure S1C). We therefore proceeded with its structural and biochemical characterization.

Structure of Borealin 207−280. We used multidimensional heteronuclear NMR spectroscopy to determine the solution structure of the soluble and folded C-terminal fragment of Borealin 207−280 (Figure 2, Table 1). As suggested by the biochemical data, we find that the C-terminal domain of Borealin is dimeric in solution, based on distance restraints between unambiguously assigned protons that can only be fulfilled in a dimeric arrangement. Furthermore, we were able to observe directly intermolecular distances between the subunits using a ^{13}C-filtered, ^{13}C-edited NOESY experiment.

Residues 226−277 of the two subunits are well-defined by the NMR-derived restraints and are arranged in a symmetric, antiparallel manner to form an elongated but compact structure. The N-terminal residues (207−225), as well as the C-terminus (residues 278−280), are conformationally undefined in the calculated structures as a result of the lack of long-range restraints. Furthermore, analysis of heteronuclear NOE data shows increased backbone dynamics for these regions of the protein (Supporting Information Figure S2).

Each monomer is composed of a pair of β-strands (β1, residues 227−233; β2, residues 237−242) that are connected by a glycine-rich turn, followed by two helices (α1, residues 248−253; α2, residues 256−274) (Figure 2). The shorter helix α1 folds back on top of the β-strands. Hydrophobic residues stabilize the interface between α1 and β1/ β2 (Supporting Information Figure S3A). Helix α2 is connected to α1 by a short linker and placed next to α1 and β1 in an antiparallel orientation.

The base of the dimer is formed by an interaction of the two β-strands of each subunit, resulting in a concavely shaped, continuous, four-stranded β-sheet (Figure 2B). Strand β1 forms the inner strand, pairing with the equivalent strand of the other subunit on one side and with the outer strand β2 of the same subunit on the other side. L229 in β1 is the cross-strand partner of the symmetry-related L229′ in the β1′ strand of the other subunit (Supporting Information Figure S3B).

The top of the Borealin 207−280 dimer is composed of the two long antiparallel α2 helices. Hydrophobic residues at the inner face of the helices, namely, L259, I262, L265, and L269, interact with residues in the neighboring α2 helix and the β1 strand of the other subunit, stabilizing the dimer interface (Supporting Information Figure S3B). In addition, L269, I272 in α2 and I276 make contacts with residues in the β2/α1 linker and in α1, thereby placing the end of the α2 helix on top of the α1 helix of the other subunit.

A structure database search (SSM/MSDfold tool (*34*)) using the Borealin 207−280 dimer structure as a query results in no significant hits. This suggests that the secondary structural elements assemble into an unprecedented arrangement and that Borealin 207−280 thereby represents a novel dimerization motif. Interestingly, when using the monomer as a search model, we identify the recently solved C-terminal acidic domain of TFIIEα as the closest related structure (*35*, *36*). Like the Borealin fold, it comprises two N-terminal β-strands, a helical linker, and a longer C-terminal helix arranged with the same topology. However, unlike the Borealin 207−280 dimer, the TDIIEα C-terminal domain is monomeric in solution. The TDIIEα C-terminal domain interacts with the PH domain of the p62 subunit of THIIH, mainly via its negatively charged N-terminus.

Effect of T230 Point Mutations on Borealin Dimerization. Borealin is reported to be phosphorylated, but it is not known what effect phosphorylation might have on its structure or on its association with functionally important binding partners. We noted that two previously reported phosphorylation sites occur within the Borealin 207−280 region. Residue S219, which is strictly conserved among species, has been shown to be phosphorylated during mitosis (*37*). More recently, T230 has been identified as one of four sites phosphorylated *in vitro* by Mps1 (*18*). This site is not strictly conserved in Borealin sequences, in particular, that of *Xenopus laevis* (Figure 1B). However, the equivalent residue is a serine or a threonine in all mammalian Borealins, as well as those from zebrafish and chicken. Therefore, we evaluated the effect of point mutations at S219 and T230 on the structural integrity of the Borealin 207−280 dimerization domain.

The first of these sites, S219, lies outside of the core structured region of the Borealin dimer (in the highly flexible N-terminal segment of our construct). Accordingly, mutations S219A, S219D, or S219K have no observable effect on the stability and structure of the purified domain, as indicated by the HSQC spectra of these mutants compared to that of the wild-type protein. In contrast, the second site, T230, is located in β-strand

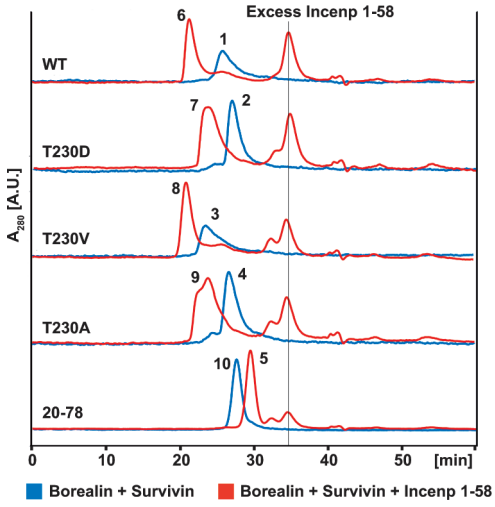

FIGURE 3: Effect of Borealin T230 point mutations on the oligomerization state of Borealin−Survivin−Incenp 1−58 complexes. Gel filtration profiles of full-length wild-type Borealin or Borealin T230 point mutants in complex with Survivin before (blue) or after (red) addition of Incenp 1−58. The bottom trace shows the same experiment with Borealin 20−78 for comparison.

1 at the dimer interface (Figure 2B) and might therefore occupy a position that is critical for the integrity of the domain. Indeed, large changes occurred in the HSQC spectra of T230A, T230D, and T230K Borealin 207−280 fragments when compared to the wild type, consistent with a substantial loss of structure. Interestingly, the same effect is observed for the phosphomimetic mutation T230D and the nonphosphorylatable T230A. Both aspartic acid and alanine residues are expected to be unfavorable for β-sheet stability (*38*), yet phosphomimetic mutants are often compared to alanine mutants to assess the functional importance of phospho sites (see, for example, ref *18*). Therefore, we designed the mutant T230V to minimally disrupt the structure of the dimer but, like T230A, to be nonphosphorylatable. We confirmed that this substitution resulted in a correctly folded Borealin 207−280 C-terminal domain by comparison of the HSQC spectra of the wild type and mutant (Supporting Information Figure S4A). We also observed an apparent increase in structural stability for the mutant, as indicated by an increase in the temperature of the midpoint of its major thermal unfolding transition (Supporting Information Figure S4B). In addition, measurement of H/D exchange by NMR indicated that the wild-type Borealin dimer (no protected amide protons) is more structurally dynamic than the T230V mutant (two protected amide protons).

To determine the effect of the T230D, T230A, or T230V substitutions on the oligomerization state of the complex of full-length Borealin with Survivin, or with both Survivin and Incenp 1−58, we compared the mobility of the relevant complexes in the gel-filtration assay described above (Figure 3 and Supporting Information Figure S5). In addition, we determined the absolute molecular size of the complexes by static light scattering (Figure 3 and Table 2).

As expected from the previously reported structures (*9*, *14*), T230 substitutions in full-length Borealin did not prevent complex formation with Survivin and Incenp 1−58. For each mutant and the wild-type Borealin, complexes elute faster upon addition of Incenp 1−58, which indicates that the change in oligomerization State of the Survivin−Borealin complex (2:2 to 1:1:1) occurs only for the smaller constructs of Borealin lacking the C-terminal domain. Second, gel-filtration profiles of complexes containing

Table 2: Observed Molecular Weights Determined by Static Light Scattering[a]

components	Bor FL WT	Bor FL T230V	Bor. FL T230D	Bor FL T230A	Bor 20−78
			Observed M_w by Light Scattering for Different Borealin Forms		
Borealin + Survivin	81 ± 0.8	86 ± 1.4	44 ± 2.5	54 ± 1.3	58 ± 0.9
Borealin + Survivin + Incenp 1−58	97 ± 0.7	114 ± 0.4	66 ± 1.0	68 ± 1.1	36 ± 1.1
			Deduced Stoichiometry (Deviation from Theoretical M_w)		
Borealin + Survivin	2 + 2 (−18.7%)	2 + 2 (−13.7%)	1 + 1 (−11.6%)	1 + 1 (+8.4%)	2 + 2 (+11.5%)
Borealin + Survivin + Incenp 1−58	2 + 2 + 2 (−14.6%)	2 + 2 + 2 (+0.4%)	1 + 1 + 1 (+16.2%)	1 + 1 + 1 (+19.7%)	1 + 1 + 1 (−9.1%)

[a] Molecular weights of full-length Borealin, Borealin 20−78, full-length Survivin, and Incenp 1−58 are 31.3, 7.5, 18.5, and 7.0 kDa, respectively. Theoretical molecular masses of complexes containing full-length Borealin are 49.8 kDa for 1:1, 56.8 kDa for 1:1:1, 99.6 kDa for 2:2, and 113.6 kDa for 2:2:2. Deduced stoichiometries for the different complexes are consistent with the gel-filtration retention volumes, indicating that complexes containing Borealin T230D and T230A are monomeric in solution.

full-length Borealin T230D or T230A mutants show that these complexes elute later than those containing full-length wild-type Borealin or the T230V mutant, consistent with a shift to a smaller average complex size.

A more detailed view emerged from the light scattering analysis. Complexes containing full-length wild-type Borealin or T230V have molecular weights corresponding to a stoichiometry of 2:2 or 2:2:2 (before or after addition of Incenp, respectively), whereas complexes containing Borealin T230D and T230A have molecular weights corresponding to a stoichiometry of 1:1 or 1:1:1 (Table 2). There are deviations of the observed molecular weights of the Borealin−Survivin−Incenp 1−58 complexes from the theoretical values (Table 2). For the wild-type Borealin complex, we observe a significant negative deviation of the observed molecular weight, suggesting an equilibrium between monomeric and dimeric complexes in fast exchange. For Borealin T230V, the very minor negative deviation of the observed molecular weight indicates that the complex is mostly dimeric, consistent with a stabilizing effect from the substitution. For Borealin T230D and T230A, the positive deviations of the observed molecular weights from 1:1:1 indicate the presence of a small population of dimeric complexes.

The observation of 1:1 Borealin−Survivin complexes indicates that higher order association (as observed for binary complexes that contain only the Borealin N-terminus) does not occur as readily in binary complexes prepared from full-length T230D or T230A Borealin. Oligomerization of Survivin in complex with short N-terminal fragments of Borealin is most likely due to a nonspecific interaction of the coiled-coil domain of each complex. Evidence for this has been observed in the crystal packing of the Borealin−Survivin binary complex (*14*). In any case, such complexes lacking Incenp are unable to localize during any stage of mitosis and thus are unlikely to be functionally relevant (*9*). Taken together, our observations on the effect of the T230 point mutations in the context of the C-terminal domain (see above) can be extrapolated to the full-length protein, identifying the Borealin C-terminal domain as the only dimerization motif within full-length Borealin.

Phosphorylation of the Borealin−Survivin Complex by Mps1. We asked whether previously described Mps1 phosphorylation sites on GST−Borealin (*18*) are also phosphorylated in the Borealin−Survivin complex. In addition, we wondered whether the T230V mutation that stabilizes the Borealin dimer would have any impact on Mps1 phosphorylation at other sites. Therefore, we treated purified wild-type and T230V complexes with Mps1 kinase domain before analysis by targeted MS/MS mass spectrometry (Supporting Information Table S1).

First, we confirmed that wild-type Borealin is phosphorylated at the previously described sites T88, T94, T169, and T230 when present in complex with Survivin. However, in contrast to the previous report (*18*) we did not recover peptides indicating simultaneous phosphorylation of T88 and T94, but instead we observed only one or the other. We also found a new phosphorylation site, S238, but this was phosphorylated at lower levels. Interestingly, analysis of the Borealin T230V complex revealed only one phosphorylation site at T94. Phosphorylation of T169 and S238 was abolished, suggesting that the dimeric form of Borealin might be a poor substrate for Mps1. In the case of wild-type Borealin, the fast exchange between the monomeric and dimeric forms may allow Mps1 to phosphorylate the monomer. In turn, Mps1 may regulate Borealin function by unfolding the C-terminal domain and/or shifting the population to the monomeric form.

Effect of T230 Mutations during Mitosis. The functional importance of Mps1 phosphorylation sites on Borealin was assessed previously by simultaneous mutation of T88, T94, T169, and T230 to alanine (4A) or to aspartic acid residues (4D). When Mps1 and endogenous Borealin were knocked down, introduction of the 4A mutant resulted in chromosome alignment defects. In contrast, introduction of the 4D mutant, which mimics a constitutively phosphorylated state, partially rescued the observed chromosome alignment defect (*18*). Because Borealin dimerization is quite sensitive to mutation at T230, we wondered whether cellular phenotypes observed for the 4A mutants were mainly due to the effect of T230A.

HeLa cells were transfected with eGFP-tagged full-length wild-type Borealin or mutants. We first observed that all transfected Borealin mutants were expressed equivalently and localized correctly during the cell cycle: we observed nuclear localization during interphase, presence at the centromeres during metaphase, transfer to the spindle midzone in anaphase, and finally concentration at the midbody during cytokinesis. Importantly, endogenous Aurora B and Survivin were also correctly localized during all stages of mitosis in the presence of overexpressed wild-type eGFP−Borealin or any of the mutant forms (Figure 4A). Mps1-depleted cells present chromosome segregation defects in anaphase and telophase (*18*). We looked for this particular phenotype after transfection of Borealin to assess the effect of T230 point mutants compared to 4A and 4D (Figure 4C). We observed 15% of cells to have lagging chromosomes in our control (eGFP transfected cells), consistent with the high chromosomal instability of HeLa cells. Cells transfected with wild-type Borealin display a slightly increased percentage of defective cells (23%), which might be explained by overexpression

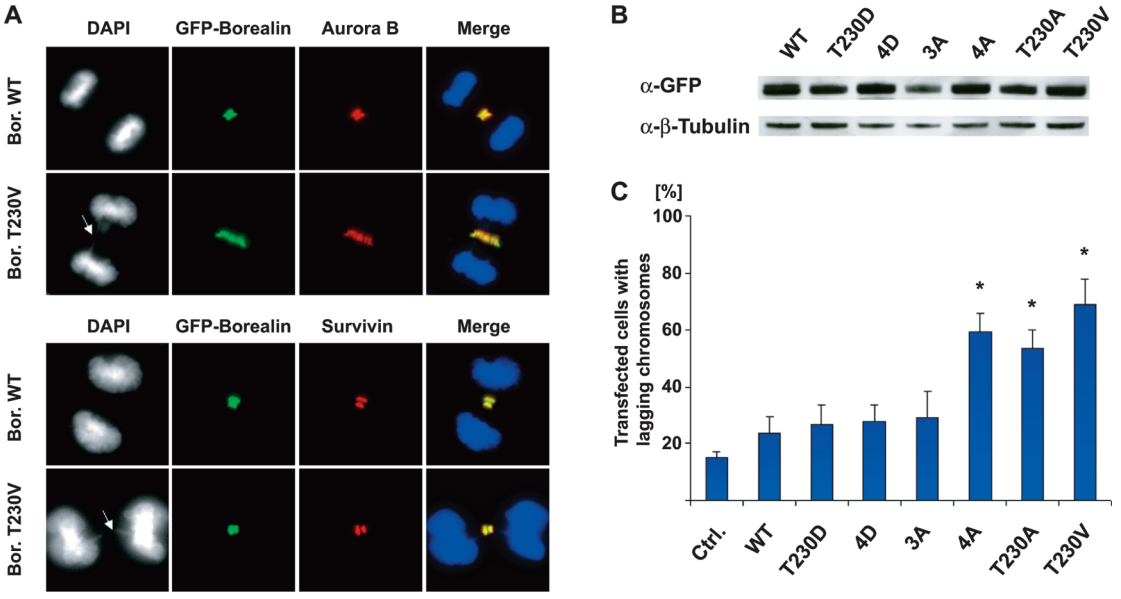

FIGURE 4: Effect of Borealin T230 point mutations on chromosome segregation. (A) Visualization of wild-type GFP−Borealin or the T230V mutant and immunostaining of Aurora B and Survivin in HeLa cells. Wild-type Borealin and the T230V mutant colocalize as expected with Aurora B and Survivin. White arrows indicate lagging chromosomes in anaphase and telophase. (B) Expression level of transfected wild-type GFP−Borealin and mutants in HeLa cells determined by Western blot. (C) Percentage of transfected (GFP-positive) cells with lagging chromosomes in anaphase or telophase. Cells transfected with Borealin mutant 4A, T230A, and T230V result in a significant increase in chromosome segregation defects compared to the cells transfected with wild-type Borealin ($p < 0.0001$; Student's t test; $n = 95$).

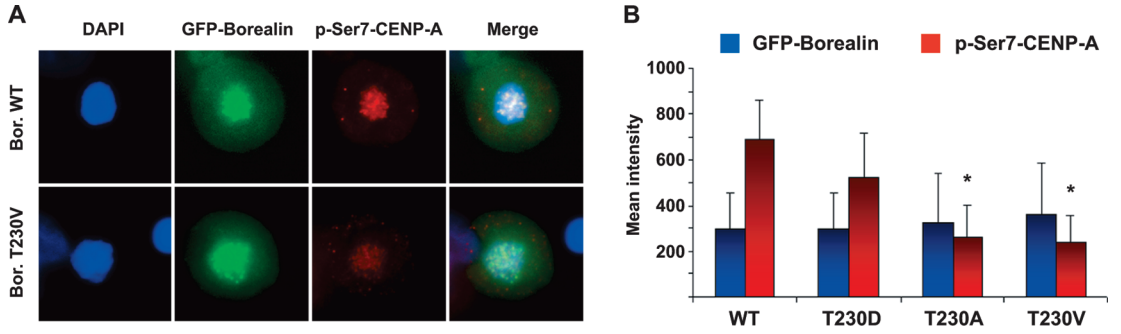

FIGURE 5: Effect of Borealin T230 point mutations on phosphorylation of CENP-A Ser7 by Aurora B. (A) Visualization of wild-type GFP−Borealin or the T230V mutant and immunostaining of endogenous p-Ser7-CENP-A in nocodazole-treated cells. (B) Nuclear mean signal intensity average of p-Ser7-CENP-A and Borealin wild type or mutants in nocodazole-treated HeLa cells (see Materials and Methods for details of quantification). Phosphorylation of CENP-A by Aurora B in cells transfected with Borealin T230A or T230V is decreased significantly ($p < 0.0001$; Student's t test; $n = 23$) compared to cells transfected with wild-type Borealin.

of the protein. Interestingly, mutation of T88, T94, and T169 to alanine (3A mutant) does not lead to a significant increase in chromosome segregation defects compared to the wild type, while, as reported previously (*18*), Borealin 4A does. Consistent with our observation of an important structural role for T230, transfection of T230A produces a defect as strong as 4A. Taken together, these data indicate that phosphorylation at T88, T94, and T169 is not necessary to promote proper chromosome alignment and that the functionally important phosphorylation site is T230. As might be expected from published data on the 4D mutant (*18*), we see little or no increase in chromosome segregation defects in cells transfected with Borealin T230D or 4D compared to those transfected with the wild-type protein. Finally, we do see a large increase in chromosome segregation defects in cells transfected with T230V; the percentage of defects is similar to that seen upon transfection of T230A.

To determine whether the effect of T230 mutations is due to an effect on Aurora B activity (*18*), we transfected wild-type eGFP Borealin or Borealin mutants and assessed the phosphorylation level of the Aurora B substrate CENP-A in nocodazole-blocked HeLa cells (*18*, *39*). A qualitative comparison of cells expressing wild type and T230V can be made by examination of images shown in Figure 5A. Because the differences in p-Ser7-CENP-A immunostaining are subtle, chromatin-associated Borealin and p-Ser7-CENP-A signal intensity was quantified after subtraction of the cytoplasmic background (Figure 5B). We observe a significant diminution of p-Ser7-CENP-A levels when Borealin mutants T230A and T230V are overexpressed. In contrast, there is relatively little effect of the T230D mutation on Aurora B activity. Therefore, as described previously for Borealin 4A (*18*), the chromosome segregation defects we observe with Borealin T230A (or T230V) are likely due to negative regulation of Aurora B activity. A straightforward hypothesis is that this regulation is direct. The phosphorylated (or unphosphorylated) C-terminal domain of Borealin might interact with Aurora B to activate (or inhibit) the kinase. However, when we added wild-type or mutant Borealin fragments (up to 12 μM) to Aurora B *in vitro* kinase reactions, we could detect no differences in activity

(data not shown). This suggests that the lower levels of phosphorylated CENP-A observed in the presence of nonphosphorylatable Borealin mutants (Figure 5) result from a less direct modulation of Aurora B activity.

DISCUSSION

In the present study, we define the C-terminal region of Borealin as a previously unrecognized dimerization motif. An NMR structure of the domain shows that it has a fold distinct from structurally characterized protein dimers. Additional biochemical studies indicate that the Borealin dimer is highly dynamic and therefore likely to exist in rapid equilibrium between monomeric and dimeric forms. Interestingly, deletion of the C-terminal half of Borealin indicates that this region is required for correct localization of the protein to the nucleolus in interphase cells (*4*) and to the centromeres during metaphase (*4*, *9*). On the other hand, a Borealin fragment containing the C-terminal motif but lacking the N-terminal helix (necessary for binding to Survivin and Incenp) fails to localize during mitosis yet localizes correctly during interphase (*4*). These data show that the Borealin C-terminal region is necessary and sufficient for localization of the protein in interphase. In addition, these data show that the same region is necessary but not sufficient for localization of the CPC to the centromeres during metaphase and that it is not required for CPC localization in anaphase and cytokinesis. However, we observe that single-site Borealin mutants that destabilize the structure of the C-terminal domain do not mislocalize during interphase or any stage of mitosis, indicating that Borealin dimerization through the C-terminal motif we have characterized here is not required for localization of the protein.

Mps1 is a kinase important for maintenance of the spindle assembly checkpoint in the presence of microtubule destabilizing drugs. Surprisingly, Mps1 was recently reported to play an additional role in chromosome alignment by promoting the destabilization of incorrect microtubule kinetochore attachments (*18*), an activity reminiscent of that of Aurora B. In the published study, Borealin was found to be an *in vitro* substrate of Mps1, and four major phosphorylation sites on Borealin (88, 94, 169, and 230) were identified (*18*). Simultaneous mutation of these four residues to alanine caused a decrease in Aurora B kinase activity, as evidenced by a decreased level of phospho-CENP-A in nocodazole-treated cells and an increased percentage of cells having lagging chromosomes at anaphase. One of these sites, T230, is present at the dimer interface of the Borealin C-terminal domain. Significantly, we observe that the defects reported for the 4A mutant can be recapitulated by the single substitutions T230A or T230V. How might substitution at this single site disrupt chromosome alignment and produce the observed segregation defects?

Physical distance of Aurora B from its substrates has been shown recently to be an important factor by which the CPC can sense interkinetochore tension and regulate microtubule attachment (*40*). In particular, the level of phospho-CENP-A is significantly higher at incorrectly attached kinetochores, while phosphorylation of a centromere-targeted Aurora B activity sensor remains relatively constant, regardless of attachment status (*40*). This suggests that the catalytic activity of Aurora B is not regulated by interkinetochore tension or kinetochore attachment to spindle microtubules; it further suggests that the higher levels of phospho-CENP-A that we and others (*18*) observe upon Borealin phosphorylation by Mps1 (or upon phosphomimetic mutation) might reflect instead a relatively shorter kinetochore−inner centromere distance and, therefore, lesser interkinetochore tension. Our inability to observe modulation of Aurora B catalytic activity *in vitro* by purified Borealin T230 mutants is consistent with this idea. Therefore, the role of Mps1 in regulating Aurora B function through Borealin might be to oppose generation of tension by tightening the connection between the CPC and the kinetochore, or, in other words, phospho-T230 Borealin might act as a resistor to forces generated by the spindle.

In the spindle checkpoint Mps1 is required to recruit Mad1 and Mad2 to kinetochores (*41*, *42*) and, very likely therefore (*43*), for production of the mitotic checkpoint complex (MCC), an inhibitor of the anaphase promoting complex (APC). Furthermore, Aurora B and Bub1 each enhance MCC inhibition of the APC (*44*). Finally, Mps1 is degraded rapidly in budding yeast by the activated APC/Cdc20 upon anaphase onset (*45*). Combining these elements with the observations discussed above, a model can be proposed which unifies physical and biochemical sensing of tension at the centromeres.

Under low tension, Mps1 is closer to the CPC at the inner centromeres and phosphorylates Borealin, helping to maintain close proximity of Aurora B and kinetochore substrates. This produces two effects: destabilization of microtubule attachments and enhancement of APC inhibition through the MCC. A positive feedback loop results by stabilization of Mps1, continued phosphorylation of Borealin T230, and maintenance of an apparently lower tension state. Therefore, the SAC response is reinforced, preventing anaphase entry. When chromosomes are under sufficiently strong tension, the resistance from phospho-T230 Borealin is overcome. This creates a negative feedback loop in which physical separation of Mps1 from Borealin helps to relieve APC inhibition, resulting in the rapid degradation of Mps1 and anaphase entry. Disruption of Borealin T230 phosphorylation through mutagenesis might be expected to weaken the connection between the CPC and its kinetochore substrates and decrease the efficiency of this feedback system, consistent with the substantial segregation defects observed.

Our results clearly show the importance of T230 for Borealin function within the CPC and support the conclusion that this residue is the functionally important Mps1 phosphorylation site. Interestingly, both dimer disruption (T230A) and dimer stabilization (T230V) produce strong segregation defects and a decrease in p-Ser7-CENP-A levels upon nocodazole treatment. In contrast, the phosphomimetic (and monomeric) form T230D produces much lesser effects. This suggests that the importance of phosphorylation is not simply to regulate a dimer−monomer equilibrium within the CPC. Furthermore, the mild defects seen with the T230D mutant suggest that dynamic phosphorylation and dephosphorylation may be relatively unimportant. Instead, it would appear that the phosphorylated form is necessary for proper chromosome alignment. One possibility is that phospho-T230 Borealin has a functionally important (and currently unidentified) binding partner. Candidates might include CPC domains not present in the constructs used in our experiments (for example, the long central region of Incenp) but could also include any of the proteins present in the cellular structures to which the CPC is targeted during early mitosis. A prediction of the "resistor" model proposed above is that phosphorylated Borealin (but not the unphosphorylated protein) should interact with some component of the kinetochore.

In considering the biological relevance of the Borealin dimer, an analogy can be made to the case of Survivin. Purified Survivin forms a homodimer in solution, but it was found several years later to be a monomer when in complex with other CPC components (*9*, *14*). Nevertheless, the region of Survivin that forms the dimerization interface is an important binding surface (for Borealin), and it adopts a similar conformation as a dimer and within the CPC. Our data do not define a clear function for the dimeric form of the Borealin C-terminal domain, although it may represent a "resting state". However, Borealin, like Survivin, may dimerize only in the absence of its intracellular partner. In this case, the dimerization interface we observe may be the region of Borealin that binds to its functionally relevant interactor, perhaps in the kinetochore. Although we cannot at present define this fully, the structural characterization of this important Borealin domain will facilitate further investigation of its function.

ACKNOWLEDGMENT

We thank Mike Elliott for assistance with static light scattering analysis and Meredith Sagolla for help with microscopy data processing.

SUPPORTING INFORMATION AVAILABLE

Targeted tandem mass spectrometry analysis of Mps1 phosphorylation sites of Borealin−Survivin complexes, characterization of Borealin C-terminal constructs, dynamics of Borealin 207−280, side chain interactions in Borealin 207−280, biophysical characterization of wild-type Borealin 207−280 and the T230V mutant, and purity of Borealin binary and ternary complexes used for stoichiometry determinations. This material is available free of charge via the Internet at http://pubs.acs.org.

REFERENCES

1. Nicklas, R. B. (1997) How cells get the right chromosomes. *Science 275*, 632–637.
2. Lens, S. M., Vader, G., and Medema, R. H. (2006) The case for Survivin as mitotic regulator. *Curr. Opin. Cell Biol. 18*, 616–622.
3. Ruchaud, S., Carmena, M., and Earnshaw, W. C. (2007) Chromosomal passengers: conducting cell division. *Nat. Rev. Mol. Cell Biol. 8*, 798–812.
4. Gassmann, R., Carvalho, A., Henzing, A. J., Ruchaud, S., Hudson, D. F., Honda, R., Nigg, E. A., Gerloff, D. L., and Earnshaw, W. C. (2004) Borealin: a novel chromosomal passenger required for stability of the bipolar mitotic spindle. *J. Cell Biol. 166*, 179–191.
5. Honda, R., Korner, R., and Nigg, E. A. (2003) Exploring the functional interactions between Aurora B, INCENP, and Survivin in mitosis. *Mol. Biol. Cell 14*, 3325–3341.
6. Vader, G., Kauw, J. J., Medema, R. H., and Lens, S. M. (2006) Survivin mediates targeting of the chromosomal passenger complex to the centromere and midbody. *EMBO Rep. 7*, 85–92.
7. Bishop, J. D., and Schumacher, J. M. (2002) Phosphorylation of the carboxyl terminus of inner centromere protein (INCENP) by the Aurora B kinase stimulates Aurora B kinase activity. *J. Biol. Chem. 277*, 27577–27580.
8. Sessa, F., Mapelli, M., Ciferri, C., Tarricone, C., Areces, L. B., Schneider, T. R., Stukenberg, P. T., and Musacchio, A. (2005) Mechanism of Aurora B activation by INCENP and inhibition by hesperadin. *Mol. Cell 18*, 379–391.
9. Jeyaprakash, A. A., Klein, U. R., Lindner, D., Ebert, J., Nigg, E. A., and Conti, E. (2007) Structure of a Survivin-Borealin-INCENP core complex reveals how chromosomal passengers travel together. *Cell 131*, 271–285.
10. Klein, U. R., Nigg, E. A., and Gruneberg, U. (2006) Centromere targeting of the chromosomal passenger complex requires a ternary subcomplex of Borealin, Survivin, and the N-terminal domain of INCENP. *Mol. Biol. Cell 17*, 2547–2558.
11. Chantalat, L., Skoufias, D. A., Kleman, J. P., Jung, B., Dideberg, O., and Margolis, R. L. (2000) Crystal structure of human Survivin reveals a bow tie-shaped dimer with two unusual alpha-helical extensions. *Mol. Cell 6*, 183–189.
12. Muchmore, S. W., Chen, J., Jakob, C., Zakula, D., Matayoshi, E. D., Wu, W., Zhang, H., Li, F., Ng, S. C., and Altieri, D. C. (2000) Crystal structure and mutagenic analysis of the inhibitor-of-apoptosis protein Survivin. *Mol. Cell 6*, 173–182.
13. Verdecia, M. A., Huang, H., Dutil, E., Kaiser, D. A., Hunter, T., and Noel, J. P. (2000) Structure of the human anti-apoptotic protein Survivin reveals a dimeric arrangement. *Nat. Struct. Biol. 7*, 602–608.
14. Bourhis, E., Hymowitz, S. G., and Cochran, A. G. (2007) The mitotic regulator Survivin binds as a monomer to its functional interactor Borealin. *J. Biol. Chem. 282*, 35018–35023.
15. Lens, S. M., Rodriguez, J. A., Vader, G., Span, S. W., Giaccone, G., and Medema, R. H. (2006) Uncoupling the central spindle-associated function of the chromosomal passenger complex from its role at centromeres. *Mol. Biol. Cell 17*, 1897–1909.
16. Yue, Z., Carvalho, A., Xu, Z., Yuan, X., Cardinale, S., Ribeiro, S., Lai, F., Ogawa, H., Gudmundsdottir, E., Gassmann, R., Morrison, C. G., Ruchaud, S., and Earnshaw, W. C. (2008) Deconstructing Survivin: comprehensive genetic analysis of Survivin function by conditional knockout in a vertebrate cell line. *J. Cell Biol. 183*, 279–296.
17. Sampath, S. C., Ohi, R., Leismann, O., Salic, A., Pozniakovski, A., and Funabiki, H. (2004) The chromosomal passenger complex is required for chromatin-induced microtubule stabilization and spindle assembly. *Cell 118*, 187–202.
18. Jelluma, N., Brenkman, A. B., van den Broek, N. J., Cruijsen, C. W., van Osch, M. H., Lens, S. M., Medema, R. H., and Kops, G. J. (2008) Mps1 phosphorylates Borealin to control Aurora B activity and chromosome alignment. *Cell 132*, 233–246.
19. Chu, M. L., Chavas, L. M., Douglas, K. T., Eyers, P. A., and Tabernero, L. (2008) Crystal structure of the catalytic domain of the mitotic checkpoint kinase Mps1 in complex with SP600125. *J. Biol. Chem. 283*, 21495–21500.
20. Delaglio, F., Grzesiek, S., Vuister, G. W., Zhu, G., Pfeifer, J., and Bax, A. (1995) NMRPipe: a multidimensional spectral processing system based on UNIX pipes. *J. Biomol. NMR 6*, 277–293.
21. Vranken, W. F., Boucher, W., Stevens, T. J., Fogh, R. H., Pajon, A., Llinas, M., Ulrich, E. L., Markley, J. L., Ionides, J., and Laue, E. D. (2005) The CCPN data model for NMR spectroscopy: development of a software pipeline. *Proteins 59*, 687–696.
22. Zwahlen, C., Legault, P., Vincent, S. J. F., Greenblatt, J., Konrat, R., and Kay, L. E. (1997) Methods for measurement of intermolecular NOEs by multinuclear NMR spectroscopy: Application to a bacteriophage lambda N-peptide/boxB RNA complex. *J. Am. Chem. Soc. 119*, 6711–6721.
23. Cornilescu, G., Delaglio, F., and Bax, A. (1999) Protein backbone angle restraints from searching a database for chemical shift and sequence homology. *J. Biomol. NMR 13*, 289–302.
24. Neri, D., Szyperski, T., Otting, G., Senn, H., and Wuthrich, K. (1989) Stereospecific nuclear magnetic resonance assignments of the methyl groups of valine and leucine in the DNA-binding domain of the 434 repressor by biosynthetically directed fractional ^{13}C labeling. *Biochemistry 28*, 7510–7516.
25. Ruckert, M., and Otting, G. (2000) Alignment of biological macromolecules in novel nonionic liquid crystalline media for NMR experiments. *J. Am. Chem. Soc. 122*, 7793–7797.
26. Rieping, W., Habeck, M., Bardiaux, B., Bernard, A., Malliavin, T. E., and Nilges, M. (2007) ARIA2: automated NOE assignment and data integration in NMR structure calculation. *Bioinformatics 23*, 381–382.
27. Brunger, A. T., Adams, P. D., Clore, G. M., DeLano, W. L., Gros, P., Grosse-Kunstleve, R. W., Jiang, J. S., Kuszewski, J., Nilges, M., Pannu, N. S., Read, R. J., Rice, L. M., Simonson, T., and Warren, G. L. (1998) Crystallography & NMR system: A new software suite for macromolecular structure determination. *Acta Crystallogr. D 54*, 905–921.
28. Linge, J. P., Williams, M. A., Spronk, C. A., Bonvin, A. M., and Nilges, M. (2003) Refinement of protein structures in explicit solvent. *Proteins 50*, 496–506.
29. Laskowski, R. A., Rullmannn, J. A., MacArthur, M. W., Kaptein, R., and Thornton, J. M. (1996) AQUA and PROCHECK-NMR: programs for checking the quality of protein structures solved by NMR. *J. Biomol. NMR 8*, 477–486.
30. Koradi, R., Billeter, M., and Wuthrich, K. (1996) MOLMOL: a program for display and analysis of macromolecular structures. *J. Mol. Graphics 14*, 51–55.
31. Zhou, L., Li, J., George, R., Ruchaud, S., Zhou, H. G., Ladbury, J. E., Earnshaw, W. C., and Yuan, X. (2009) Effects of full-length Borealin

on the composition and protein-protein interaction activity of a binary chromosomal passenger complex. *Biochemistry 48*, 1156–1161.
32. Schultz, J., Milpetz, F., Bork, P., and Ponting, C. P. (1998) SMART, a simple modular architecture research tool: identification of signaling domains. *Proc. Natl. Acad. Sci. U.S.A. 95*, 5857–5864.
33. Biegert, A., Mayer, C., Remmert, M., Soding, J., and Lupas, A. N. (2006) The MPI Bioinformatics Toolkit for protein sequence analysis. *Nucleic Acids Res. 34*, W335–339.
34. Krissinel, E., and Henrick, K. (2004) Secondary-structure matching (SSM), a new tool for fast protein structure alignment in three dimensions. *Acta Crystallogr. D 60*, 2256–2268.
35. Di Lello, P., Miller Jenkins, L. M., Mas, C., Langlois, C., Malitskaya, E., Fradet-Turcotte, A., Archambault, J., Legault, P., and Omichinski, J. G. (2008) p53 and TFIIEalpha share a common binding site on the Tfb1/p62 subunit of TFIIH. *Proc. Natl. Acad. Sci. U.S.A. 105*, 106–111.
36. Okuda, M., Tanaka, A., Satoh, M., Mizuta, S., Takazawa, M., Ohkuma, Y., and Nishimura, Y. (2008) Structural insight into the TFIIE-TFIIH interaction: TFIIE and p53 share the binding region on TFIIH. *EMBO J. 27*, 1161–1171.
37. Nousiainen, M., Sillje, H. H., Sauer, G., Nigg, E. A., and Korner, R. (2006) Phosphoproteome analysis of the human mitotic spindle. *Proc. Natl. Acad. Sci. U.S.A. 103*, 5391–5396.
38. Distefano, M. D., Zhong, A., and Cochran, A. G. (2002) Quantifying beta-sheet stability by phage display. *J. Mol. Biol. 322*, 179–188.
39. Zeitlin, S. G., Shelby, R. D., and Sullivan, K. F. (2001) CENP-A is phosphorylated by Aurora B kinase and plays an unexpected role in completion of cytokinesis. *J. Cell Biol. 155*, 1147–1157.
40. Liu, D., Vader, G., Vromans, M. J., Lampson, M. A., and Lens, S. M. (2009) Sensing chromosome bi-orientation by spatial separation of Aurora B kinase from kinetochore substrates. *Science 323*, 1350–1353.
41. Abrieu, A., Magnaghi-Jaulin, L., Kahana, J. A., Peter, M., Castro, A., Vigneron, S., Lorca, T., Cleveland, D. W., and Labbe, J. C. (2001) Mps1 is a kinetochore-associated kinase essential for the vertebrate mitotic checkpoint. *Cell 106*, 83–93.
42. Tighe, A., Staples, O., and Taylor, S. (2008) Mps1 kinase activity restrains anaphase during an unperturbed mitosis and targets Mad2 to kinetochores. *J. Cell Biol. 181*, 893–901.
43. Musacchio, A., and Salmon, E. D. (2007) The spindle-assembly checkpoint in space and time. *Nat. Rev. Mol. Cell Biol. 8*, 379–393.
44. Morrow, C. J., Tighe, A., Johnson, V. L., Scott, M. I., Ditchfield, C., and Taylor, S. S. (2005) Bub1 and Aurora B cooperate to maintain BubR1-mediated inhibition of APC/CCdc20. *J. Cell Sci. 118*, 3639–3652.
45. Palframan, W. J., Meehl, J. B., Jaspersen, S. L., Winey, M., and Murray, A. W. (2006) Anaphase inactivation of the spindle checkpoint. *Science 313*, 680–684.
46. Cornilescu, G., Marquardt, J. L., Ottiger, M., and Bax, A. (1998) Validation of protein structure from anisotropic carbonyl chemical shifts in a dilute liquid crystalline phase. *J. Am. Chem. Soc. 120*, 6836–6837.
47. Jeanmougin, F., Thompson, J. D., Gouy, M., Higgins, D. G., and Gibson, T. J. (1998) Multiple sequence alignment with Clustal X. *Trends Biochem. Sci. 23*, 403–405.